Received: 7 July 2020 | Revised: 19 February 2021 | Accepted: 27 February 2021

DOI: 10.1002/joc.7081

RESEARCH ARTICLE

International Journal of Climatology RMetS

Building a local climate reference dataset: Application to the Abruzzo region (Central Italy), 1930–2019

Gabriele Curci[1,2] | **Jose A. Guijarro**[3] | **Ludovico Di Antonio**[1] | **Mario Di Bacco**[4] | **Bruno Di Lena**[5] | **Anna Rita Scorzini**[3]

[1]Dipartimento di Scienze Fisiche e Chimiche, Università degli Studi dell'Aquila, L'Aquila, Italy

[2]Center of Excellence in Telesensing of Environment and Model Prediction of Severe events (CETEMPS), Università degli Studi dell'Aquila, L'Aquila, Italy

[3]Agencia Estatal de Meteorologia (AEMET), Delegación Territorial en Illes Balears, Palma De Mallorca, Spain

[4]Dipartimento di Ingegneria Civile, Edile – Architettura, Ambientale, Università degli Studi dell'Aquila, L'Aquila, Italy

[5]Centro Agrometeorologico Regionale, Regione Abruzzo, Italy

Correspondence
Gabriele Curci, Dipartimento di Scienze Fisiche e Chimiche, Università degli Studi dell'Aquila, L'Aquila, Italy.
Email: gabriele.curci@univaq.it

Abstract

Reliable secular time series of essential climatic variables are a fundamental element for the assessment of vulnerability, impact and adaptation to climate change. Here, we implement a readily portable procedure for building an upgradable long-term homogeneous climate dataset using monthly and daily observations of temperature and precipitation over a given area of interest, exemplified here with Abruzzo, a region in Central Italy characterized by complex orography. We process the dataset according to a preliminary ranking of stations based on data quantity and quality, and we exploit the Climatol algorithm for inhomogeneity correction. The corrected time series show trends in broad agreement with external databases (CRU, Berkeley Earth, E-OBS), and highlight the importance of relying on a local network for a better representation of gradients and variability over the territory. We estimate that maximum (TX) and minimum temperature (TN) increased by ~1.6 and ~2.2°C/century, respectively, over the period 1930–2019, while in the recent decades 1980–2019 we found an accelerated trend of ~5.7 and ~3.9°C/century. Precipitation (RR) decreased by ~10%/century in 1930–2019, while it has been increasing at a rate of ~26%/century in 1980–2019. The Köppen–Geiger climate classification is sensitive to the increase of precipitation in the recent decades, which is attributable to decreased summer precipitation overcompensated by more rain in late spring and early autumn. The cold climate types are retreating upwards along the slopes of the mountain ranges. Over the period 1980–2019, extreme values are also displaying significant trends. Every 2 years, there is one less frost day (TN <0°C) and one more summer day (TX >25°C) in the Apennines area, while there is one more tropical night (TN >20°C) in the Adriatic coastal area. Precipitation extremes are increasing, especially along the coast, with rain accumulated in the rainiest days increasing at a rate of 1–2%/year.

Abbreviations: BER, Berkley Earth; CAR, Centro Agrometeorologico Regionale; CRU, climate research unit; CSV, comma separated values (a common ASCII file format); ISPRA, Istituto Superiore per la Protezione e la Ricerca Ambientale (Higher Institute for Environmental Protection and Research); QC, quality check; RR, accumulated precipitation; TM, mean temperature; TN, minimum temperature; TX, maximum temperature; UIM, Ufficio Idrografico e Mareografico della Regione Abruzzo (Hydrographic and Mareographic Office of the Abruzzo Region).

KEYWORDS

climate change detection indices, climate classification, climate time series, climate trend, homogenization

1 | INTRODUCTION

Reliable climate time series from near-surface observational networks are the backbone of any climate service, that is, the ensemble of data and information products aimed at supporting the response of society to climate change and climate-related risks (Brasseur and Gallardo, 2018). The historical time series, after proper treatment for correcting inhomogeneities due to station drift, substitution and relocation (Brunetti *et al*., 2006; Ribeiro *et al*., 2016), are used to obtain a detailed picture of the climate state and its trend in the region of interest (Peel *et al*., 2007; Brunetti *et al*., 2014). The same kind of dataset is the basic input for regional climate statistical downscaling (Maraun, 2016) and the necessary validation reference for dynamical downscaling (Giorgi, 2019).

Several datasets collecting meteorological observations from stations around the globe or a continent have been developed in recent decades. Despite rigorous control protocols, also products such as the widely used E-OBS dataset (Cornes *et al*., 2018) may present distortions, with respect to more densely distributed and controlled local networks, which may have significant repercussions in the results of downstream applications (Hofstra *et al*., 2009; Kyselý and Plavcová, 2010).

A comprehensive review of temperature and precipitation trends in the last century in the Abruzzo region, which is the focus area of this work, and its consistency with trends in the Mediterranean basin and the rest of Italy, may be found in Scorzini and Leopardi (2019). The Mediterranean basin is often considered a climate 'hot spot', because of its vulnerability against even small changes in climate dynamics. Indeed, the basin is at the interface between the arid tropical (Northern Africa) and the rainy mid-latitude (continental Europe) climate regimes, and thus a relatively small change in the cyclonic and anticyclonic synoptic patterns may result in substantial modifications to for example, the regional precipitation distribution in both space and time (Guijarro *et al*., 2006; Giorgi and Lionello, 2008).

Similarly to most places on the globe, temperature in Italy has been found to have increased in the last century, with a trend of the order of 1°C/century: in Central and Southern Italy, minimum temperature increased at a rate of about 1.3°C/century, about twice as much as the 0.7°C/century of maximum temperature (Brunetti *et al*., 2006). A similar increasing trend was reported also for the Abruzzo region, where Aruffo and Di Carlo (2019) estimated a 20-fold mean temperature increasing rate from ~0.3°C/century in the period 1924–1979 to ~6.0°C/century in 1980–2015, in line with the nation-wide study by Fioravanti *et al*. (2019). The extreme temperature indices are also displaying significant trends in the recent decades: for example, on average, in the Abruzzo region the number of 'summer days' (maximum temperature TX higher than 25°C) is increasing by one every year, and the number of 'frost days' (minimum temperature TN less than 0°C) is decreasing by one every 2 years (Scorzini *et al*., 2018).

Regarding precipitation, Brunetti *et al*. (2006) estimated a generally decreasing trend of the mean annual precipitation over Italy in the last century, while the seasonal precipitation trend showed a variable sign also depending on the area of interest (Caporali *et al*., 2021). For what concern Southern Italy, annual precipitation is decreasing by about −104 mm/century, mostly attributable to a reduction in spring and autumn months (Brunetti *et al*., 2000). In Abruzzo, Scorzini and Leopardi (2019) found precipitation trends in the eastern coastal area of the region amplified compared to the western mountainous part (see Figure 1 for a map of the topography of the region). The long-term trends of mean annual precipitation in the period 1951–2012 are similar in the two areas (−160 mm/century and −136 mm/century, respectively in the coastal and the mountainous cluster), while the estimated rates are −290 mm/century in 1951–1981 and +540 mm/century in 1982–2012 for the coastal area, and −77 mm/century and +226 mm/century, respectively, in the mountainous area. The increasing precipitation trend in the recent decades was found in all seasons, in particular in spring and autumn. Summer precipitation was found to increase also in the long-term (+16 mm/century in 1951–2012), but the rate has been slowing down in the recent decades (+160 mm/century in 1951–1981 and +11 mm/century in 1982–2012).

In this work, we implement a procedure to quality check (QC), homogenize and facilitate the continuous update of the climate dataset of the Abruzzo region in Central Italy. The procedure is solely based on publicly available software and information and it could be readily applied to other regions of interest around the globe. The manuscript is organized as follows. Firstly, we illustrate the raw dataset and the selected combination of existing methods applied for QC and correction of inhomogeneities. Secondly, we display the results of the homogenization procedure and compare results with

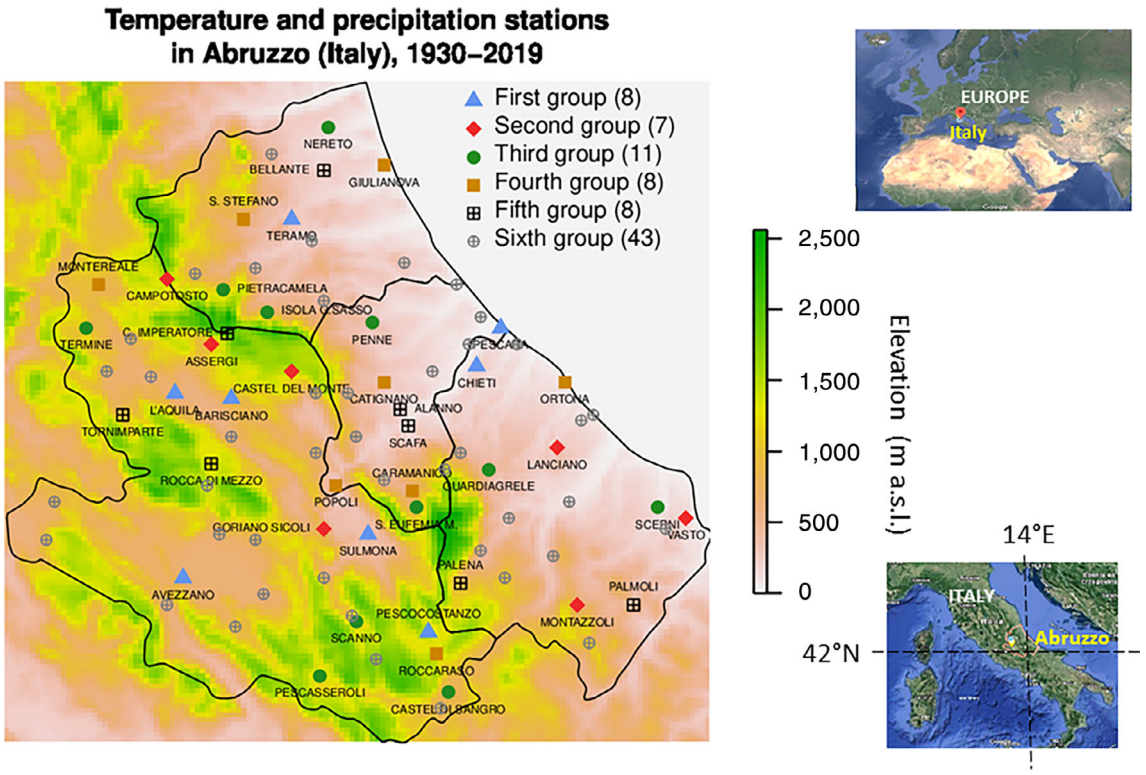

FIGURE 1 Location of temperature and precipitation stations used in this study focused on the Abruzzo region in Central Italy (the position of the region is illustrated inn the Google Maps insets on the right; the whole region is contained approximately in a 130 km × 130 km box). The stations are divided in six groups according to data quantity and quality, for homogenization purposes (see text and Table 1 for details) [Colour figure can be viewed at wileyonlinelibrary.com]

other gridded datasets (CRU, Berkeley Earth, E-OBS) and with past work on the same raw dataset used here. Then, we incrementally analyse the dataset in order to gather a consistent picture of the climate over the region and its change in the last century (since 1930). We begin with maps of the long-term annually average temperature and precipitation and the illustration of estimated trends throughout the period. We also use the Köppen–Geiger classification to illustrate the signal of climate change contained into the observations. Finally, we further specialize the picture focusing on the daily time series starting in 1980, employing Walter–Lieth diagrams and extreme climate indices as analysis tools.

2 | DATA AND METHODS

2.1 | Abruzzo region ground-based weather database

The list of stations considered in this study is displayed in Table 1 and Figure 1. We use the observations of temperature and precipitation over the Abruzzo region collected by the sensors network, distributed over about 200 locations, managed by the regional public Hydrographic and Mareographic Office (Ufficio Idrografico e Mareografico, Regione Abruzzo, https://www.regione.abruzzo.it/content/idrografico-mareografico, denoted 'UIM' afterwards). UIM delivers its digitized database on request for research purposes. We selected only stations measuring both temperature and precipitation and we choose 1930 as starting year for subsequent analysis, because earlier only a few stations were available. More extensive notes on data rescue are provided in Supporting Information.

2.2 | QC procedures

We apply basic QC procedures before any attempt to pass the data through a homogenization procedure, as commonly recommended (Peterson *et al*., 1998; World Meteorological Organization, 2008). The QCs procedures are those applied by ISPRA (the national Higher Institute for Environmental Protection and Research) (Fioravanti *et al*., 2016), which in turn are derived from international standards, and are divided in two main sequential parts: the first applies to single stations, the second to group of stations. The first part is aimed at identifying non-physical values (such as unrealistically high or low

TABLE 1 List of available stations, grouped according to the class in several periods

Code	Site name	Prov	Lon.	Lat.	Alt. (m)	1930.2019	1980.2019	1930.1959	1940.1969	1950.1979	1960.1989	1970.1999	1980.2009	1990.2019
First group: At least Class C in all periods, sufficient data in 2019														
920	BARISCIANO	AQ	13.57	42.32	978	B	B	B	C	C	B	B	B	B
7710	AVEZZANO	AQ	13.45	41.99	658	B	A	B	B	B	B	A	A	A
1060	CHIETI	CH	14.18	42.38	278	B	B	B	B	B	B	B	B	B
550	L'AQUILA	AQ	13.43	42.33	595	B	B	B	B	A	A	B	B	B
1160	PESCARA	PE	14.24	42.45	5	B	C	B	B	A	B	C	B	C
1180	PESCOCOSTANZO	AQ	14.06	41.89	1,461	C	B	B	B	B	B	B	B	B
810	SULMONA	AQ	13.91	42.07	372	B	B	B	A	B	B	B	B	B
100	TERAMO	TE	13.72	42.65	218	B	B	A	B	B	B	B	B	B
Second group: At least Class C in periods 1930–2019 and 1980–2019, sufficient data in 2019														
590	ASSERGI	AQ	13.52	42.42	992	B	B	-	-	B	B	A	B	B
190	CAMPOTOSTO	AQ	13.41	42.54	1,344	B	B	A	B	B	B	B	A	-
860	CASTEL DEL MONTE	AQ	13.72	42.37	1,346	B	B	-	B	B	B	A	A	-
670	GORIANO SICOLI	AQ	13.8	42.08	958	C	C	-	B	B	B	B	C	C
1330	LANCIANO	CH	14.38	42.23	298	B	B	-	B	B	A	A	B	-
1680	MONTAZZOLI	CH	14.43	41.94	871	B	B	-	B	A	B	B	B	B
1740	VASTO	CH	14.7	42.1	196	B	C	-	B	B	A	B	C	B
Third group: At least Class C in period 1930–2019														
1420	CASTEL DI SANGRO*	AQ	14.11	41.78	800	C	C	-	B	A	B	B	A	-
1240	GUARDIAGRELE	CH	14.21	42.19	551	C	-	-	-	C	C	B	B	-
260	ISOLA DEL G.SASSO (PRETARA)*	TE	13.66	42.48	545	B	C	A	B	B	B	A	C	-
30	NERETO*	TE	13.81	42.82	165	C	B	B	A	A	C	B	B	-
380	Penne*	PE	13.92	42.46	431	B	B	B	B	A	B	B	B	A
1350	PESCASSEROLI*	AQ	13.79	41.81	1,164	C	-	-	B	A	C	B	C	-
220	PIETRACAMELA*	TE	13.55	42.52	1,043	C	C	B	B	A	A	A	C	-
970	SANT'EUFEMIA A MAIELLA*	PE	14.03	42.12	888	C	-	B	C	B	B	A	A	-
700	SCANNO*	AQ	13.88	41.91	1,039	C	-	B	C	B	B	B	A	-
1700	SCERNI*	CH	14.63	42.12	287	B	-	-	A	B	B	C	B	-
490	TERMINE*	AQ	13.21	42.45	1,031	C	-	B	B	B	B	B	C	-

TABLE 1 (Continued)

Fourth group: At least Class C in period 1980–2019														
980	CARAMANICO METEO	PE	14.02	42.15	804	-	C	-	-	-	-	-	C	B
1110	CATIGNANO	PE	13.95	42.35	334	-	B	-	-	-	-	-	B	B
50	GIULIANOVA	TE	13.95	42.75	67	-	C	-	-	-	-	-	C	C
470	MONTEREALE	AQ	13.24	42.53	913	-	B	-	-	-	-	A	B	B
1300	ORTONA	CH	14.4	42.35	75	-	B	-	-	-	-	B	B	-
850	POPOLI*	PE	13.83	42.16	250	-	B	-	-	A	A	B	B	C
1430	ROCCARASO	AQ	14.08	41.85	1,231	-	C	-	-	-	C	B	B	C
80	SANTO STEFANO	TE	13.6	42.65	820	-	B	-	-	-	-	B	B	B
Fifth group: Class D ('-') in both periods 1930–2019 and 1980–2019														
1040	ALANNO	PE	13.99	42.3	295	-	-	-	-	B	A	B	B	-
130	BELLANTE*	TE	13.8	42.74	363	-	-	-	-	-	-	-	B	B
580	CAMPO IMPERATORE	AQ	13.56	42.44	2,125	-	-	-	B	C	-	-	-	-
1570	PALENA*	CH	14.14	41.98	781	-	-	-	B	A	B	B	B	-
1870	PALMOLI*	CH	14.57	41.94	624	-	-	-	B	A	B	B	B	-
630	ROCCA DI MEZZO*	AQ	13.52	42.2	1,329	-	-	-	B	C	B	B	-	-
1010	SCAFA*	PE	14.01	42.27	88	-	-	-	-	-	-	-	B	-
520	TORNIMPARTE	AQ	13.3	42.29	873	-	-	-	-	-	-	-	B	-

Note: Stations marked with an asterisk (*) are not considered currently operational, because they do not have a sufficient number of data in 2019. The 43 stations in the sixth group (recent stations still operational with at least 5 years of data) are not listed.

temperatures, maximum temperature lower than minimum temperature, etc.) and non-physical temporal sequences of data (e.g., repeated values, abrupt jumps, etc.), while the second is mostly aimed at identifying outliers by inter-comparing values among nearby or most correlated stations. In Table S3, we list the QC tests applied to the dataset, with the number of flagged values. The test that flags more data is the check on the number of consecutive zeros for precipitation. For temperature, the most populated test is the spatial corroboration test. Overall, the number of flagged values is about 0.01–0.03% for temperature and 1.4–2.8% for precipitation. Excluding the test on the repeated series of zeros (which is usually due to erroneous transcription of missing precipitation data as zeros [Peterson *et al*., 1998]), the fraction for precipitation is similar to that of temperature. These proportions are consistent with expectations from QC procedures (Durre *et al*., 2010). For the sake of illustration, some examples of flagged data are reported in Supporting Information. We discard the flagged values from any further analysis and proceed with the homogenization procedures using the remaining values.

2.3 | Homogenization procedures and preliminary station selection

We use the homogenization procedure implemented in the R package Climatol (Guijarro, 2019). R is a free programming environment for data analysis and graphics (R Core Team, 2020). The worldwide user community delivers and maintains the quality-checked optional packages on the Comprehensive R Archive Network (CRAN). Here we employ version 3.6 of R software. The tool was chosen for two reasons: (1) it is a state-of-art automatic homogenization software and (2) it is publicly available and integrated into controlled and maintained software repositories. Moreover, in recent inter-comparison exercises (http://www.climatol.eu/MULTITEST/, (Fioravanti *et al*., 2019)), the skill of the algorithm in detecting breaks in timeseries has been shown to be similar or superior to other homogenization tools. Although a completely unsupervised homogenization procedure is not recommended (Aguilar *et al*., 2003), the implementation of these procedures in automatic and semi-automatic software packages is now common practice (Ribeiro *et al*., 2016), because most of the homogenization methods exploit lengthy iterative inter-comparisons of several nearby and correlated stations. Some basic recommendations in approaching homogenization of historical time series are (Brunetti *et al*., 2006; Ribeiro *et al*., 2016): (1) inter-compare results obtained with different methods, (2) apply corrections only when the uncertainty on the detection of the breaks is much larger than the variability of the time series, in order to avoid the introduction of even larger inhomogenities and (3) try to validate the results with independent information, such as metadata information or other reference time series. We consider these recommendations in the form illustrated below.

The working principle of Climatol is to calculate abrupt changes in the anomalies at one station with respect to the time series at the same location estimated from data collected at other stations (Guijarro, 2019). Since this procedure would require time series of the same lengths, which is not generally possible due to missing data or network restructuration in time, Climatol iteratively infill missing data from neighbouring locations, until a stable estimate of the mean is reached at each station. The series of anomalies after data imputation is then used to: (1) identify possible outliers and (2) test the homogeneity of the series applying the Standard Normal Homogeneity Test (SNHT; Alexandersson, 1986; see the Supporting Information section 3). Every time a series has a SNHT value overpassing a threshold (the default is 25, but may be adjusted by the user) the series is split in two parts at the time when the maximum SNHT is detected. The procedure is repeated iteratively, until no further inhomogeneous series is found. Moreover, since the presence of two or more breaks in a series cannot be detected by the SNHT test, the actual algorithm is devised in two phases: a first application to series regularly divided in overlapping time windows, a second application to the whole series. The data filling procedure may be applied to both daily and monthly series, without any upper limit to the length of the timeseries, but requiring a minimum of three neighbouring stations having valid data at all time-steps.

As a check on the automatic procedure, we first visually inspected the results of Climatol break detection and fine-tuned the statistical thresholds, then we compared them with the information available on station maintenance documented in UIM yearbooks, as well as with the breaks documented in the two previous studies from independent research groups that homogenized the same dataset (Aruffo and Di Carlo, 2019; Scorzini *et al*., 2018), both using the homogenization software HOMER (Mestre *et al*., 2013). The HOMER package was developed during the European COST Action ES0601 «HOME», Advances in Homogenization Methods of Climate Series: An Integrated Approach (Venema *et al*., 2012): we verified that the code is still currently available, but not updated or integrated in the CRAN (Comprehensive R Archive Network, https://cran.r-project.org/mirrors.html) since 2013. We point out that the procedures we developed are not strictly dependent on Climatol, but are modular: the homogenization part could be plugged-in with alternative

algorithms, without affecting the rest of the procedures, and this is indeed a desirable future development.

The selection of stations for the analysis appears to be always affected by some degree of subjectivity and to be dependent on the time period selected for the analysis: for example, regarding the analysis of the temperature dataset, the previous studies focused on different periods and used slightly different selection procedures, which resulted in a different mix of selected stations for the final analysis (Aruffo and Di Carlo, 2019; Scorzini *et al*., 2018; Scorzini and Leopardi, 2019). Here we build on the same criteria used in the construction and continuous update of the European ECA&D database (ECA&D, 2013), now called E-OBS and integrated in the European Copernicus service (Copernicus Climate Change Service, 2020), which requires a minimum length of 20 years of the time series and 70% of valid data over the period of interest. We further make a preliminary screening of the quality of the time series applying the four tests against the null hypothesis of homogeneity illustrated in (Wijngaard *et al*., 2003), and still currently used also for the E-OBS database (ECA&D, 2013). Based on these tests, which are illustrated in Supporting Information, each time series is independently classified as:

- Class A: the station is 'useful' for both temperature and precipitation
- Class B: the station is 'useful' for precipitation and 'doubtful' or 'suspect' for temperature
- Class C: the station is 'doubtful' or 'suspect' for both temperature and precipitation
- Class D: the station has an insufficient number of data for both temperature and precipitation

Moreover, since the final aim of the work is to build a set of reference time series which could be updated progressively in the future, we check for the presence of a sufficient number of data (at least 70% or 9 months of valid values) in the last year of the dataset (2019 in this study), to verify that the station is currently operational. The detection of significant break points is performed on the monthly time series, for both computational expediency and improved detection capability, which is more effective with less noisy data. The homogenization of the daily time series is carried out building on the monthly time series break detection: the daily series are split at the same times of the respective monthly series, and corrected series are calculated with the same data filling procedure used for monthly data.

As a final assessment, we compare our homogenized series with other international climatic reconstructions, namely: (1) the Climate Research Unit (CRU) gridded global dataset version 4.03 at $0.5^\circ \times 0.5^\circ$ resolution (Harris *et al*., 2014) (https://crudata.uea.ac.uk/cru/data/hrg/); (2) the European E-OBS gridded dataset version 20.0e at $0.1^\circ \times 0.1^\circ$ resolution (Cornes *et al*., 2018) (https://www.ecad.eu/download/ensembles/ensembles.php); (3) the Berkley Earth global gridded dataset at $1^\circ \times 1^\circ$ resolution (http://berkeleyearth.org/data/).

2.4 | Köppen–Geiger climate classification maps

We employ a spatial interpolation of station data applying the kriging method proposed by Hiemstra *et al*. (2009). The spatial distribution over the region is reasonably representative of the complexity of the territory (Figure 1): the station density tends to increase around the mountains with respect to the plain near the coast on the East. The distribution in altitude of the stations is roughly half below 500 m and half in the range 500–1,500 m. We thus employ a universal kriging interpolation using both a digital elevation model (DEM) and a land cover map as predictors. We use the EU-DEM v1.0 at 1 km × 1 km (EU-DEM, 2020), the same used as background for the map in Figure 1, and the CORINE Land Cover v2018 at 0.1 km × 0.1 km (CLC, 2018), both provided by the Copernicus Land Monitoring Service. We interpolate the station point data over the 1 km × 1 km grid of the EU-DEM, clipped on the borders of the Abruzzo region. We remap the CORINE Land Cover onto the EU-DEM grid and we collapse the original 44 land cover categories into the 8 proposed by the Land and Ecosystem Accounting (European Environment Agency, 2006) as used by Lai *et al*. (2020). We acknowledge this is a first reference version of the maps, which could potentially be further improved with additional auxiliary variables such as distance to the coastline and satellite products (Vicente-Serrano *et al*., 2017; Beguería *et al*., 2018; Baronetti *et al*., 2020), but we leave these possible revisions for future development.

We use the interpolated monthly dataset to illustrate the change in the climate zones in the Abruzzo region. A widely used climate zone clustering is the Köppen–Geiger classification, originally proposed by (Köppen, 1884) and updated until recently (Kottek *et al*., 2006; Peel *et al*., 2007), which has been demonstrated to provide a compact basic picture of the climate state and evolution in many disciplines. We follow the procedure of Peel *et al*. (2007), which relies on the calculation of the following indices: mean annual temperature (*T*ann) and precipitation (*P*ann), the mean monthly temperature of the coldest (*T*cold) and hottest (*T*hot) month, the number of months in a year with mean temperature higher than 10°C (*T*mon10), the mean monthly precipitation of the driest (*P*dry) month, the mean precipitation of the driest and wettest months in summer

and winter (*P*sdry/*P*swet, *P*wdry/*P*wwet). In Supporting Information, we report the criteria for the selection of the climate types found in our dataset, while for the complete list the reader is referred to Peel *et al*. (2007).

2.5 | ETCCDI climate extremes indices

In addition to the mean climate state and trend, we provide a first overview of the trends of indices of extreme climate events, exploiting the daily time series. We employ the indices recommended by the Expert Team on Climate Change Detection and Indices (ETCCDI, 1999). In particular, we show for temperature: the number of days with TX and TN less than the 10th percentile (TX10p and TN10p), the number of days more than 90th percentile (TX90p and TN90p), the number of frost days (FD, TN <0°C), the number summer days (SU, TX >25°C), the number of tropical nights (TR, TN >20°C), and the growing season length (GSL, period with daily mean temperature >6°C). For precipitation: the maximum precipitation in 1-day and 5-days events (Rx1day and Rx5day), the number of days with more than 10 and 20 mm of precipitation (R10mm and R20mm), the total precipitation above the 95th and 99th percentile of daily rain (R95pTOT and R99pTOT), and the maximum lengths in days of dry (RR <1 mm/day) and wet (RR ≥1 mm/day) spells (CDD and CWD).

3 | RESULTS

3.1 | Homogenization of time series

In Figure 2, we show the station counts in Classes A–C (please refer to Section 2.3 for details), for several selected time intervals: the two long periods of the monthly (1930–2019) and the daily (1980–2019) time series, and a progression of 30-years blocks overlapping by 10 years, spanning the whole time interval under analysis (1930–2019). The total number of stations having a sufficient number of data in at least one 30-years block is 42. This preliminary analysis of the time series highlights the general presence of inhomogeneities in the dataset; moreover, the lack of a reference station, which could be used to drive the correction of other inhomogeneous stations, motivated the use of the Climatol algorithm (Guijarro, 2019) to homogenize the time series before any further analysis, given that this tool does not necessarily require one or more reference stations. Details of the method are provided in Section 2.3.

For data analysis subsequent to time series homogenization, we divide the set of 42 stations into five groups according to their quality and quantity, as reported in Table 1 and displayed in Figure 1. The first group contains eight stations that are at least Class C in all the periods and have sufficient data in 2019. The second group is made of seven stations that are at least in Class C in both long-term periods and have sufficient data in 2019. The third (11 stations) and fourth (eight stations) groups are at least in Class C in the 1930–2019 and 1980–2019 periods, respectively. The fifth is in Class D for both long-term periods (remaining eight stations).

Climatol set breaks at times when the SNHT statistic overpass a threshold, which could be adjusted by the user. After the application of the algorithm one may look at the distribution of SNHT values found in the final set of homogeneous pieces of the time series, and check if the chosen threshold delimits more or less abruptly the tail of the distribution of SNHT values. In this way, one may decide to increase or decrease the SNHT threshold in order to obtain a sharper cut of the distribution tail. The distributions of SNHT values of the time series employed here and the related counts of breaks are reported in section 3 of Supporting Information. From visual inspection of the distributions, we selected the following SNHT thresholds: 30 for TX, 35 for TN and 25 for RR. With this SNHT values, the Climatol procedure locates a total number of breaks for the 42 stations over the period 1930–2019 equal to 236, 239 and 82 for TX, TN and RR, respectively. The sensitivity of the break detection to the input parameters and stations selection is further explored in Section 3.6.

In Figure 3 we show the yearly averaged time series for the three variables under examination (monthly values of TX, TN and RR) for 'first group' stations (see Table 1 and Figure 1). It is possible to appreciate the effect of the homogenization procedure in reducing the unrealistic oscillations in some of the original temperature timeseries and in making the trends more qualitatively comparable, with respect to the original data, to the three comparison databases (E-OBS, CRU and Berkeley Earth). While no substantial trend is evident for precipitation, the homogenized series and those of the three external databases all clearly indicate a warming trend in the region, especially after 1980. Although the time series are similar in terms of trends' shape, they substantially differ in terms of absolute values, and there might be differences of up to 5°C and 500 mm/year among the datasets. None of the datasets is systematically closer to the homogenized series for all stations and all variables. This highlights the importance of building a reliable reference from local measurements for climatic applications: for example, it may be seen how the maximum temperature is much more uniform among the stations than suggested by the global/continental databases, while

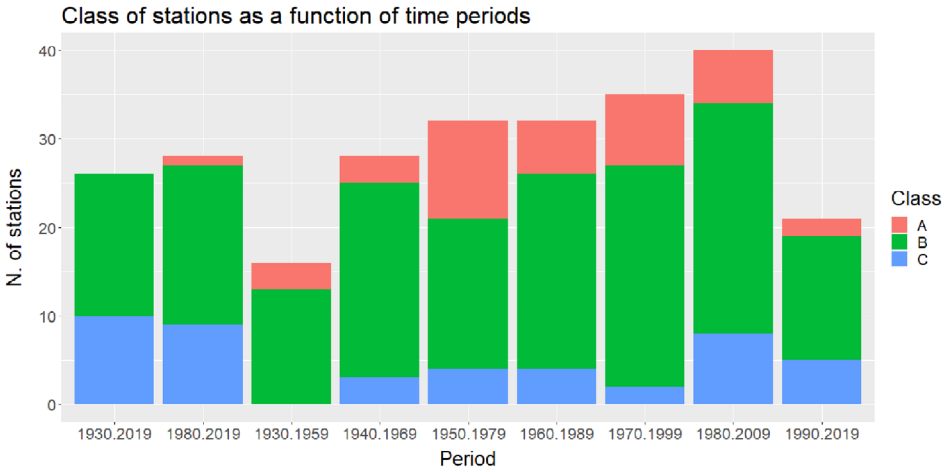

FIGURE 2 Station counts per Class in selected time periods. Classes are defined as follows: A, series is homogeneous for both temperature and precipitation; B, series is homogeneous only for precipitation; C, is inhomogeneous for both temperature and precipitation. Stations in Class D (insufficient data to assess inhomogeneity) are not shown. Please refer to text for more details [Colour figure can be viewed at wileyonlinelibrary.com]

the minimum temperature and the precipitation have much larger variability in local observations. Similar plots for stations in the other groups are given in Supporting Information.

Possible reasons for the large discrepancies among the external datasets and the local one are the number of stations used and the resolution of the dataset. To corroborate these hypotheses, we show in section 5 of Supporting Information the scatterplot of temperature and precipitation versus altitude for the different datasets. The original and homogenized local data show a relatively compact relationship, especially for maximum temperature. The CRU and EOBS database display more scatter and in general a steeper gradient for temperature and less steep gradient for precipitation with respect to local series. These observations support the hypotheses we made to explain the differences, however the issue deserves more in-depth analysis in the future.

3.2 | Definition of a static picture of the Abruzzo climate: 1930–2019

In Figure 4, we show the interpolated maps resulting from the universal kriging for mean temperature and precipitation over the period 1930–2019. The mean annual temperature (*T*ann) is estimated as the average of maximum and minimum temperature. The eastern part of the Abruzzo region, delimited by the Adriatic Sea on the East and the Apennines on the West, is a relatively homogeneous band, with a gentle east-west gradient of both temperature and precipitation: the mean annual temperature (*T*ann) decreases from 16 to 17°C along the coast to 13–14°C at the base of the Apennines, while the mean annual precipitation (*P*ann) increases from 600–700 mm/year to 900–1,000 mm/year. The western mountainous part of the region has generally lower mean temperatures and higher mean precipitation than the eastern part and is much more heterogeneous, with sharp gradients due to the complex topography. The mean annual temperature ranges from 15 to 16°C of the warmest valleys to 2–4°C of the mountain peaks. The difference of the *T*ann in the valleys with respect to the eastern part of the region is mainly due to the minimum temperature, while the maximum temperature is quite similar to that of the coast. As regards precipitation, we observe 1,400–1,500 mm/year in mountain areas, compared to the 600–800 mm/year in the valleys.

3.3 | Trends in climate mean state, 1930–2019

In Figure 5, we show the average value and the trend (slope of linear fit) calculated in 30-years blocks throughout the period 1930–2019 for TX, TN, TM and RR, averaged over the homogenized time series of stations in the first, second and third groups. TM is the mean temperature estimated as the average of TX and TN. An increasing temperature trend appears after 1960s, while in the previous years there is no clear tendency. In the last four decades, the warming rate has been around 5–6°C/century for TX and 3–5°C/century for TN. These magnitudes are consistent with trends previously reported for Italy and the Abruzzo region (Aruffo and Di Carlo, 2019; Brunetti *et al.*, 2006; Fioravanti *et al.*, 2019; Scorzini and Leopardi, 2019).

Precipitation shows a negative trend of −40%/century during the 1960s, with a difference of −60 mm/year between the periods 1955–1984 and 1965–1994, and a partial recover after 1980s, with a trend around +20%/century. A sharp decrease of precipitation over Italy after the middle of the 1900s was also found by Brunetti *et al.* (2006), while the increasing trend in recent decades was also reported by Scorzini and Leopardi (2019). The origin of these alternate trends in precipitation are an interesting feature that warrants further analysis in the future.

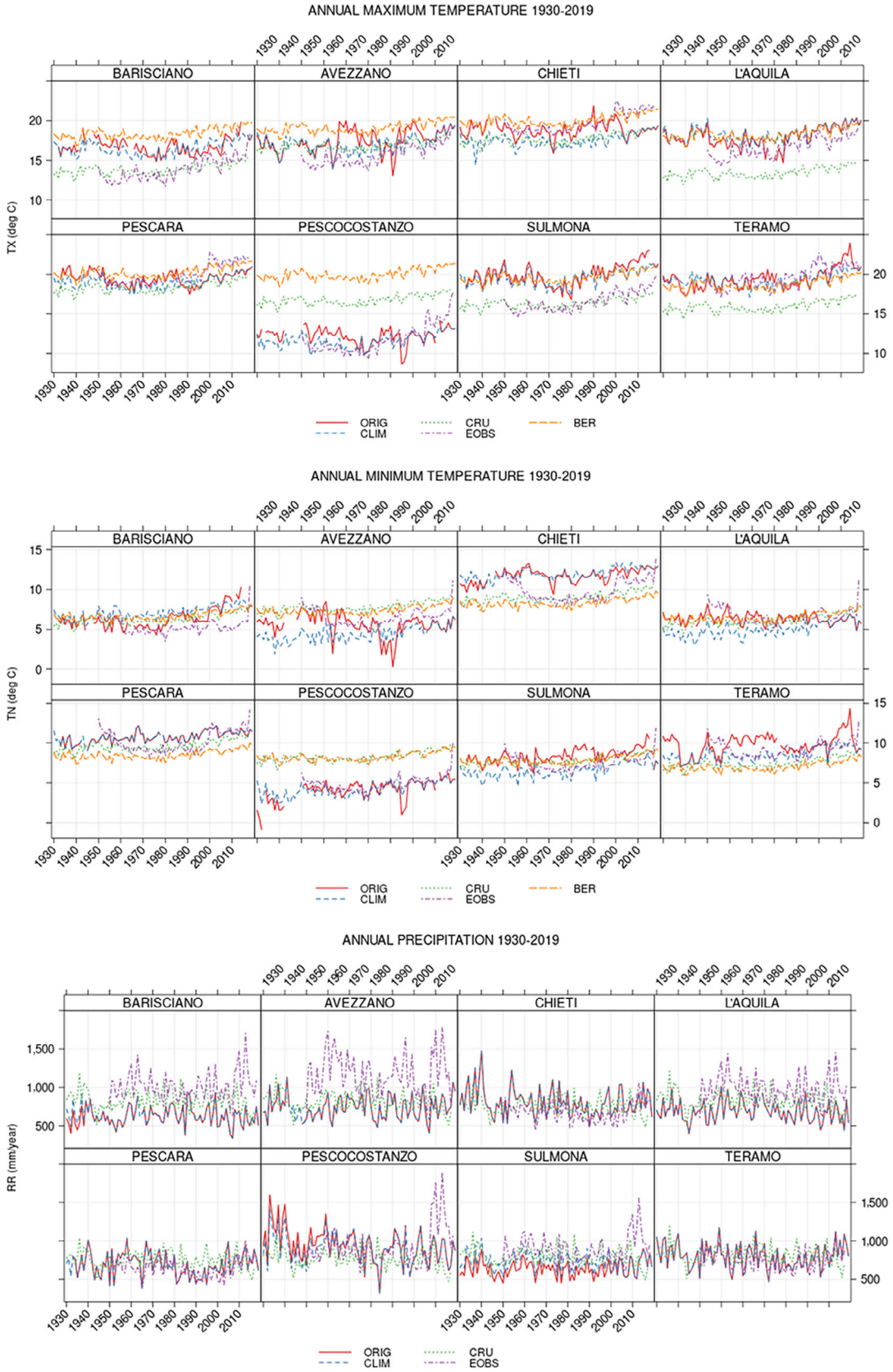

FIGURE 3 Illustration of the effect of homogenization on yearly timeseries of stations in the first group. From top to bottom: maximum temperature (TX), minimum temperature (TN), precipitation (RR). Solid lines denote the original (uncorrected) timeseries, dashed line the series homogenized using Climatol package (Guijarro, 2019). The series are also compared with those interpolated at station location from the following gridded databases: E-OBS v20.0e at 0.1° × 0.1° (EOBS, dash-dot line), climate research unit TS4.03 at 0.5° × 0.5° (CRU, dotted line), and Berkley earth at 1° × 1° (BER, long-dashed line) [Colour figure can be viewed at wileyonlinelibrary.com]

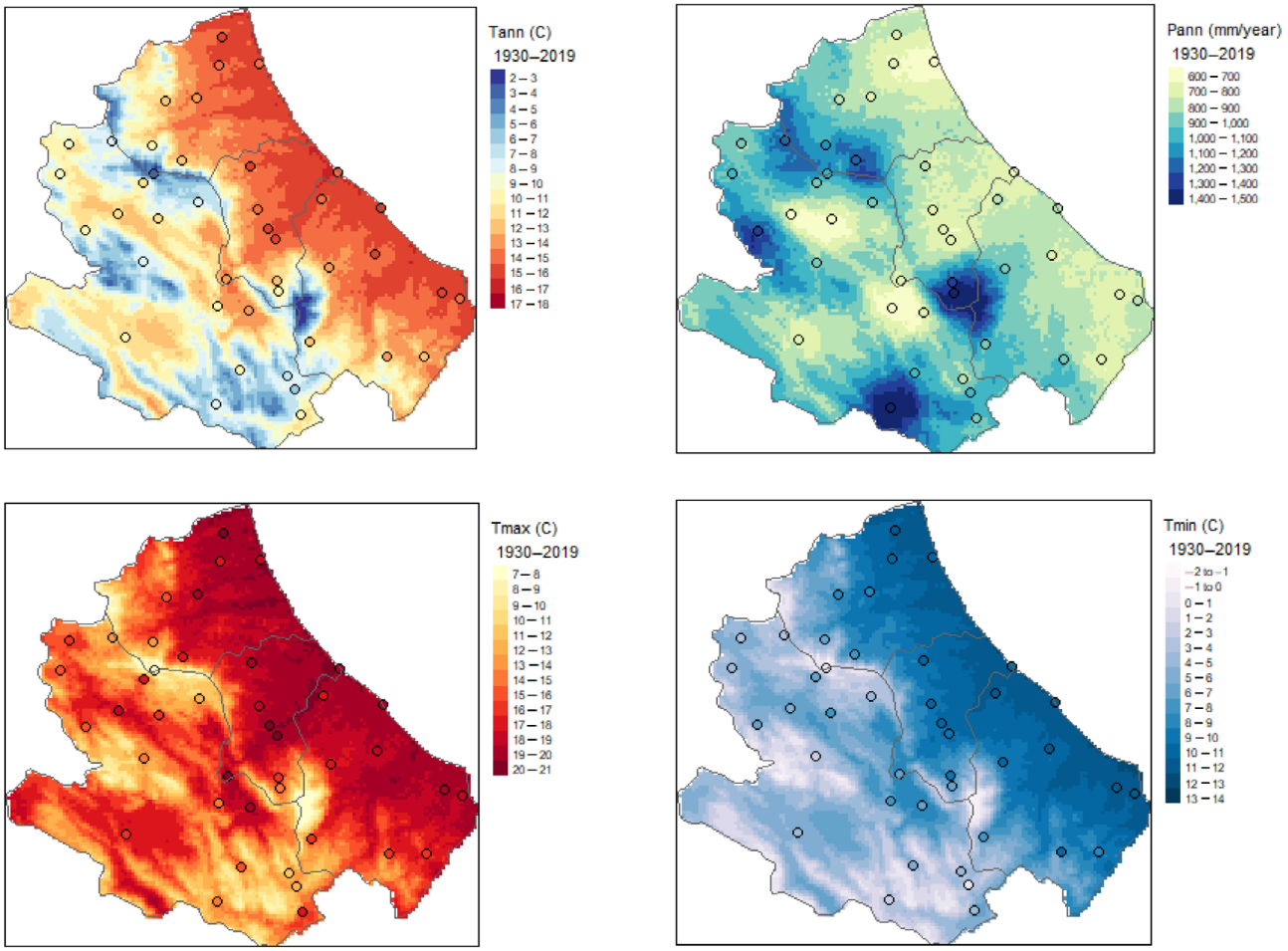

FIGURE 4 Interpolated map, using universal kriging with a digital elevation model as predictor, of mean annual temperature (top-left) and precipitation (top-right) over the Abruzzo region over the period 1930–2019. Also shown the maps for average maximum (bottom-left) and minimum (bottom-right) temperature [Colour figure can be viewed at wileyonlinelibrary.com]

In Figure 6, we compare the trends estimated from the local timeseries (both original and homogenized) and from the external databases. Trend quantification is based on the Theil-Sen slope estimate (Sen, 1968) with accompanying estimate of the 95% confidence interval (Ropkins and Carslaw, 2012). We calculate trends over the two long-term periods, 1930–2019 and 1980–2019. The original data, especially for temperature, are characterized by a wide scatter among the stations, confirming the necessity of a correction procedure for their use on climatic time scales. The homogenization procedure makes the trends much more similar among the stations, but avoiding excessive 'flattening' of the differences. The inter-station differences are larger in the 1980–2019 period than in the 1930–2019, as it might be expected from a shorter timeseries. The global databases display much less inter-station scatter, with trends that are almost identical over the region. The European database E-OBS, on the other hand, shows a scatter which is larger than the local dataset.

We note significantly different trends for the longer-term series 1930–2019 and the most recent period 1980–2019. Regarding temperatures, the minimum temperatures increased (~2.2°C/century) more than maximum temperature (~1.6°C/century) in 1930–2019, while in the 1980–2019 period the reverse has been happening (TN ~3.9°C/century vs. TX ~5.7°C/century). These tendencies are confirmed by the global and European databases, but the magnitudes are different: the global databases (CRU, Berkeley Earth) display a spatially uniform magnitude comparable to the one of the local database, while the E-OBS database exhibits larger trend slopes, with also larger spatial variability.

Regarding precipitation, both the local and the global (CRU) databases suggest a decrease (−5÷ − 10%/century) over the period 1930–2019, while in 1980–2019 the trend is reversed (23÷71%/century) in both local and European datasets, while it is still decreasing in the global CRU database. The inter-station difference is quite similar in the local and E-OBS trends, while in the lower resolution

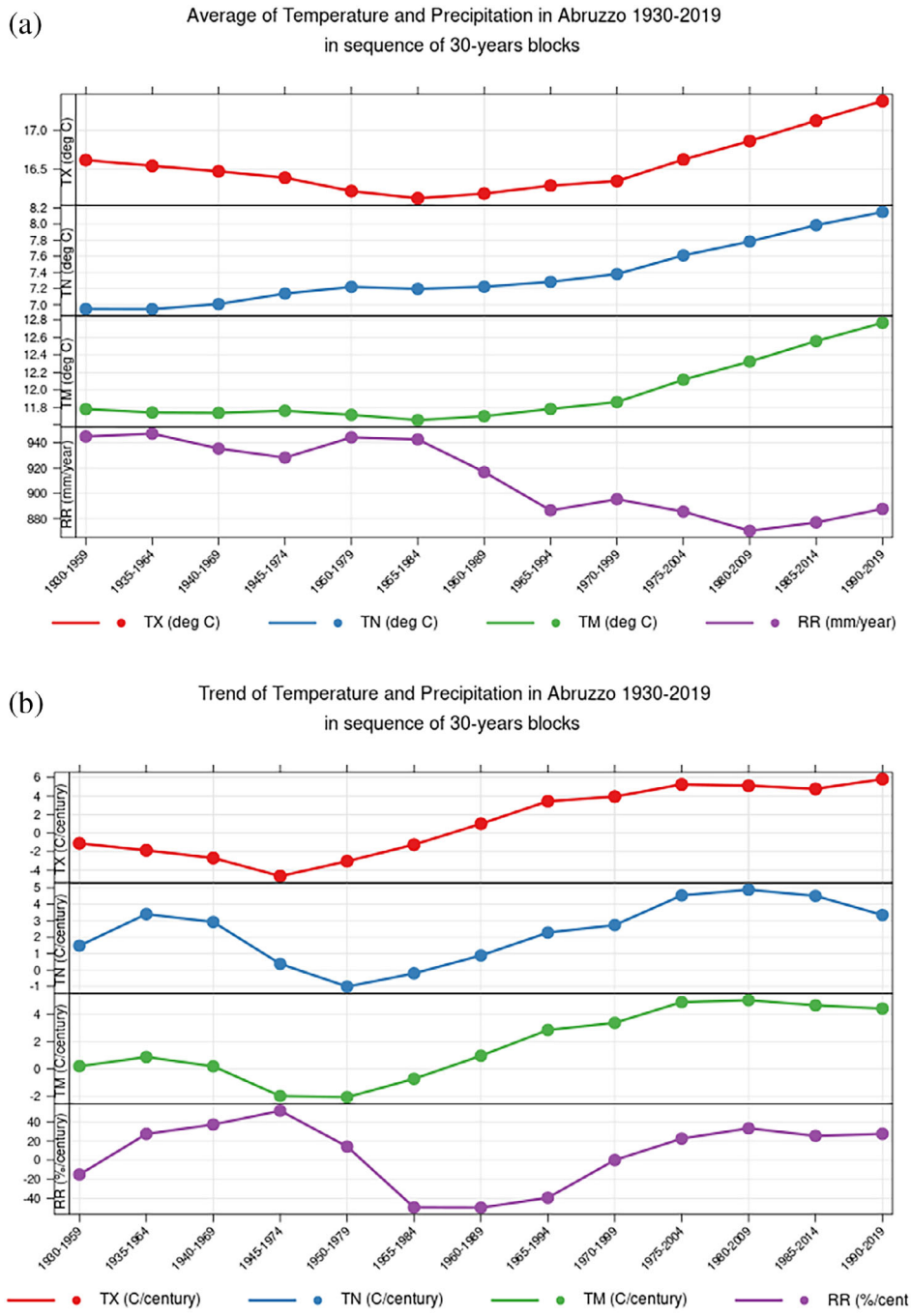

FIGURE 5 (a) Time series of average TX, TN, TM (mean temperature, calculated as [TX + TM]/2), RR over the homogenized series in blocks of 30-years in the period 1930–2019. (b) Time series of average trends of the same variables in the 30-years blocks [Colour figure can be viewed at wileyonlinelibrary.com]

CRU database there is almost no difference among stations. This again suggests that the dense station network we adopted here is desirable to represent the spatial variability of precipitation over this complex terrain region.

In Figure 7, we show the maps of the Köppen–Geiger climates in Abruzzo calculated over two sub-periods of 50 years, namely 1930–1979 and 1970–2019. The overlap is in correspondence with the marked transition we noted in Figure 5 during the years 1960–1970, where we showed a change from a flat to an increasing temperature trend, and a decrease in precipitation. In both periods, the part of Abruzzo located east of the Apennines display a prevalent Cfa climate (temperate without dry season and with hot summer), while the western part is more variable, from temperate (C*) in the valleys to cold (D*) on the mountains. Large parts of the valleys have become wetter in summer (please note that, 'summer' in the Köppen–Geiger classification includes months from April to September, see the Supporting Information), passing from climates Csa/Csb to Cfa/Cfb. Moreover, there is a retreat of the cold climates around the slopes of the mountain ranges, which shifted from Dfb to Cfb. The coldest climate Dfc around the top of the mountains does not seem to have changed much between the two periods. These features are broadly consistent with the station trends illustrated in Figure 6, but implicitly add some detail on the seasonality of the change.

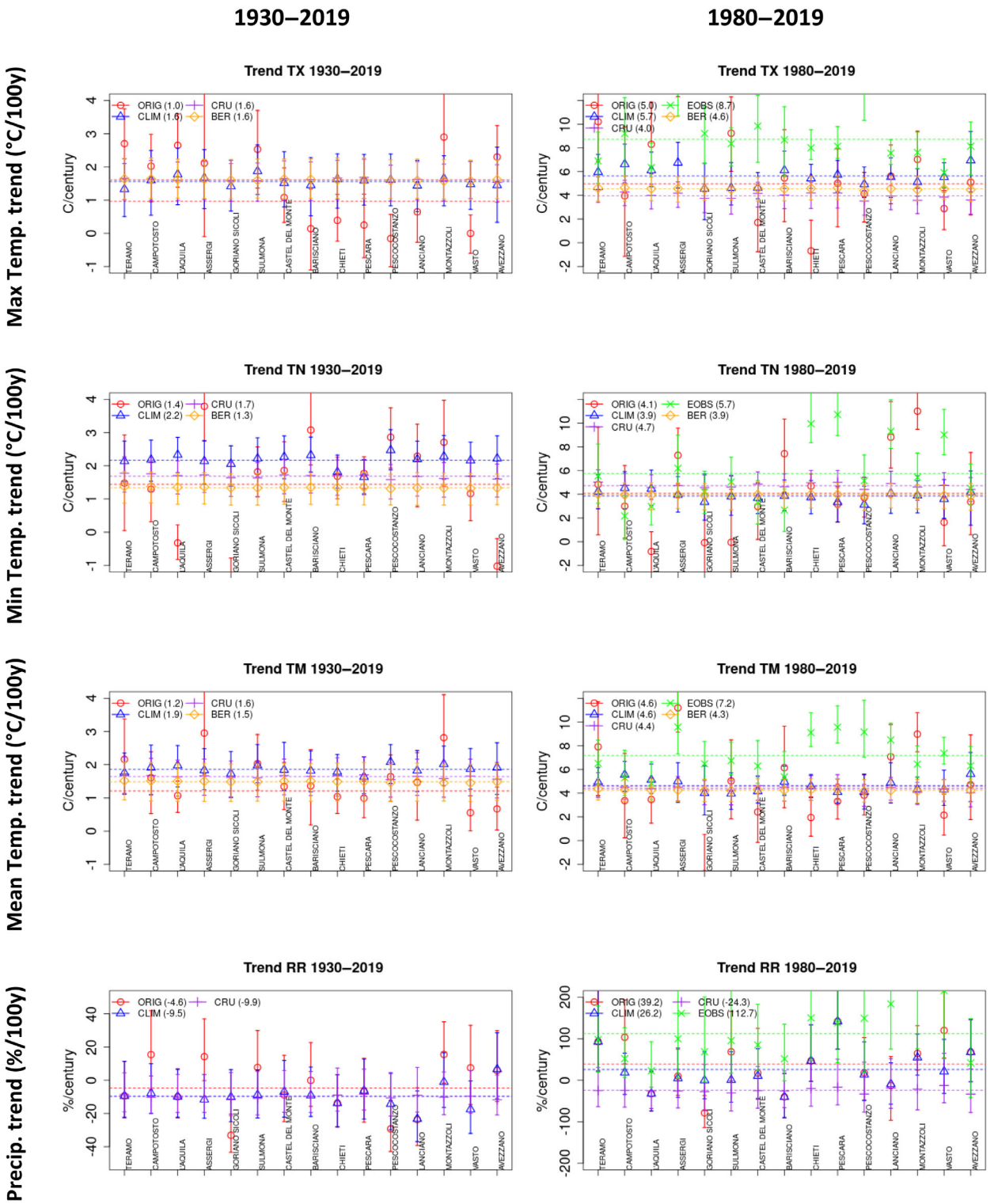

FIGURE 6 Estimated trends of monthly time series for TX, TN, TM, and RR over the periods 1930–2019 (left) and 1980–2019 (right). Original (circle) and homogenized with Climatol (triangle) series are compared with CRU (plus), Berkeley Earth (diamond) and E-OBS (cross). The uncertainty of the trends denotes the 95% confidence interval. The horizontal lines denote the station's average trend, whose numerical value is reported in parentheses in the legend. Only the 15 stations classified in the 'first' and 'second' groups are displayed [Colour figure can be viewed at wileyonlinelibrary.com]

For example, the recent precipitation trend in L'Aquila and Barisciano indicates a decrease on an annual basis, but since the precipitation in the warm part of the year slightly increased, we observe a shift from a 'dry summer' (Cs*) to a 'without dry season' (Cf*) classification, consistently to what is reported in Scorzini and Leopardi (2019). The emerging climate trend is also consistent with that illustrated by Rubel *et al.* (2017) for the Northern Apennines.

3.4 | Yearly cycles, 1980–2019

In order to illustrate the seasonal variation of mean temperature and precipitation over the region, we employ here the daily timeseries in the period 1980–2019 to construct Walter–Lieth climate diagrams (Walter and Lieth, 1967). The Walter–Lieth climate diagram shows the annual cycle of the monthly temperature and precipitation on the same graph, highlighting the 'dry', 'humid' and 'wet' periods of the year. Moreover, information is provided around the axes on the extreme values of temperature and the probability of frost days (both of which requires daily time series), plus the mean annual temperature and precipitation.

In Figure 8, we display the Walter–Lieth diagrams on the Abruzzo map at the location of the selected stations. Two illustrative examples of the information given in the diagrams are reported in the bottom part of the figure. In Abruzzo, most places along the coast and in the valleys have a dry summer period, while other seasons are humid, with the autumn being generally the wettest period. The chance of frost days is always present at least from November to April, and in the mountain valleys there is certainty of having frosts during winter. The locations along the steep slopes of the mountain ranges are the wettest and coldest places. Most of them display a wet period in autumn with no dry summer period, even if in this season the precipitation is at its minimum.

In Figure 9, we compare the Walter–Lieth diagrams of two 20-years subperiods 1980–1999 and 2000–2019, using the average data of two subset of stations: a 'dry' group collecting those with a mean annual precipitation less than 850 mm, and a 'wet' group with those with more than 850 mm. This threshold divides the stations in the valleys and the coast from those over the mountain slopes. Comparing the two periods, in both groups of stations there is an increase of 20–30 mm/year of *P*ann and a modification to the temporal distribution of monthly precipitation. Indeed, we notice a slight decrease of precipitation in summer and winter, and a more substantial increase of precipitation in spring and early autumn. The diagram of more recent years thus shows a summer minimum and a relatively homogeneous distribution of precipitation among the other seasons, with November still the rainiest month, but not as outstandingly as in the past.

3.5 | Trends of climate extremes, 1980–2019

The analysis of daily time series allows a more detailed inspections of climate trends in terms of variability around the mean values and of extremes values. We use the daily timeseries 1980–2019, and we calculate the climate indices elaborated by ETCCDI (1999, see section 2.5).

In Figure 10, we show the estimated trends of the ETCCDI indices related to temperature extremes, averaging the stations in two groups: 'Apennines', which includes the stations in the western mountainous part of the region and 'Coast', which includes the stations along the sea in the eastern part of Abruzzo. For TX and TN percentiles, the trend is similar all over the region: the

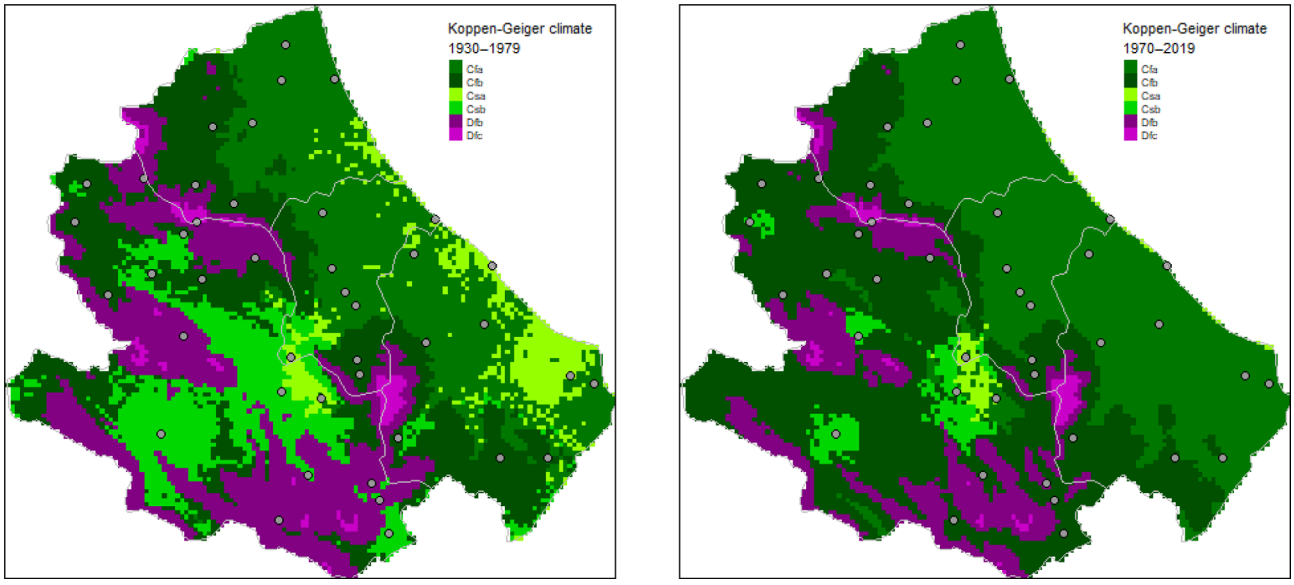

FIGURE 7 Köppen–Geiger climate types estimated from the interpolated homogenized temperature and precipitation monthly series in the Abruzzo region. Two periods are compared: 1930–1979 on the left and 1970–2019 on the right. The dots denote the position of the stations used as basic data for the implementation of the maps [Colour figure can be viewed at wileyonlinelibrary.com]

number of days below the 10th percentile is decreasing at a rate of about −0.25 per year, while the number of days above the 90th percentile is increasing at a rate of about 0.25 per year. In the 'Apennines' area, frost days are decreasing at a rate of −1 day every 2 years, while summer days are increasing at a rate of 1 day every

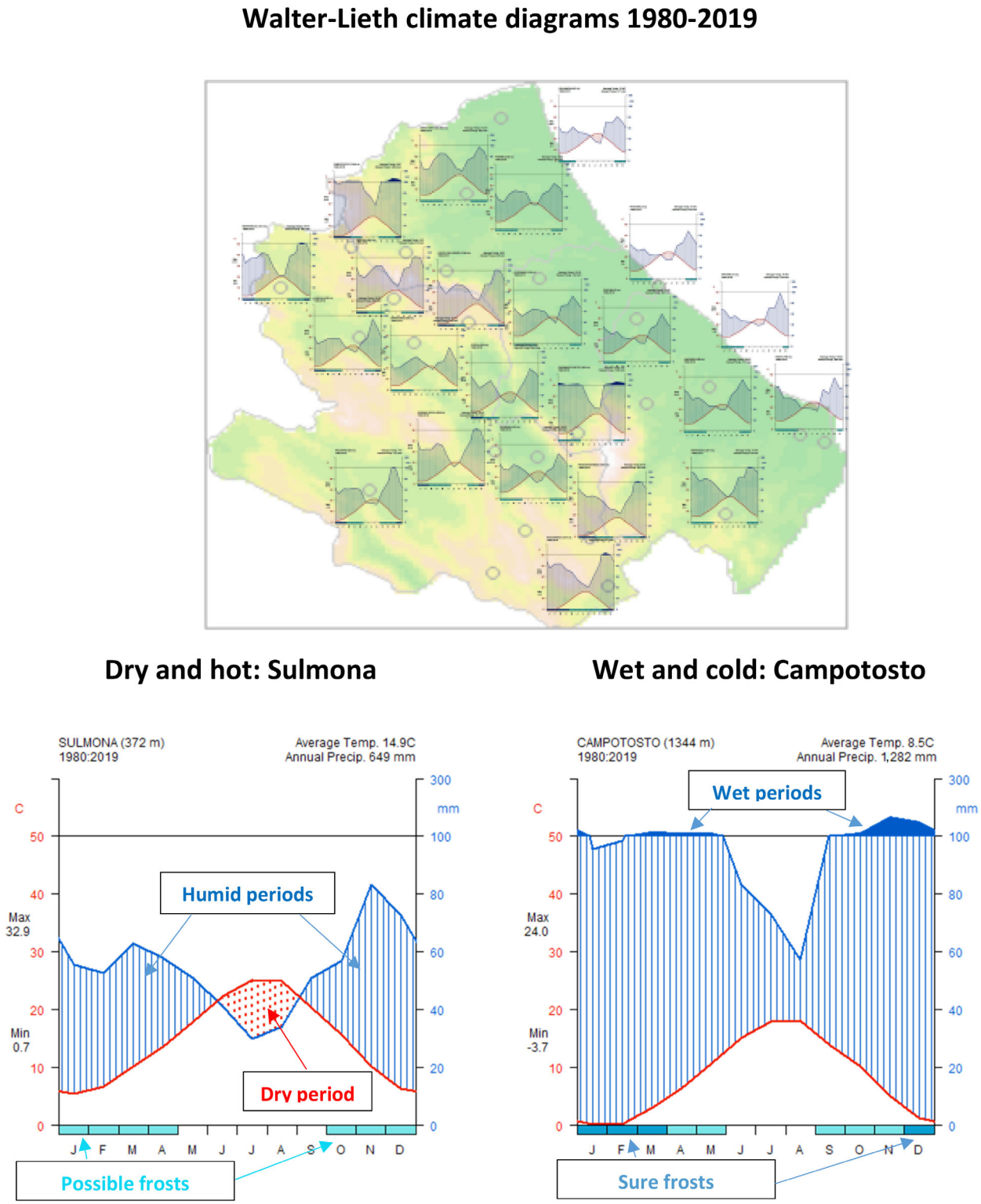

FIGURE 8 Map of Walter–Lieth climate diagrams on the Abruzzo map for the stations in the first, second, and fourth groups over the period 1980–2019. In the two bottom panels two exemplificative diagrams of one of the drier and hotter (Sulmona) and one of the wetter and colder (Campotosto) locations [Colour figure can be viewed at wileyonlinelibrary.com]

2 years. The GSL also shows a positive trand, with duration increasing by more than 1 day every year, and catching up with the GSL on the 'Coast' area. In the 'Coast' area, the number of summer days is increasing at a rate of 1 every 3 years, and tropical nights by 1 every 2 years.

In Figure 11, we show the precipitation-related ETCCDI indices. The recent increasing trend of precipitation in the region is accompanied also by a positive trend of its extremes, especially in the 'Coast' area. There, the accumulated rain in 1-day and 5-days events is increasing, with a statistically significant trend of about 0.6 and 0.9 mm/year, respectively. The number of days with rain higher than 10 and 20 mm used to be higher in the 'Apennines' area in the 1980s, but the 'Coast' is slowly catching up at a pace of 0.05–0.1 days/year. The precipitation accumulated in the rainiest days (R95PTOT and R99PTOT) is also increasing significantly in the 'Coast' area, at a rate of about 2–3 mm/year, while there is no significant trend in the 'Apennines' area. The length of dry spells (CDD) has no significant trend, while the length of wet spells (CWD) is slightly increasing both in the 'Apennines' and the 'Coast' area.

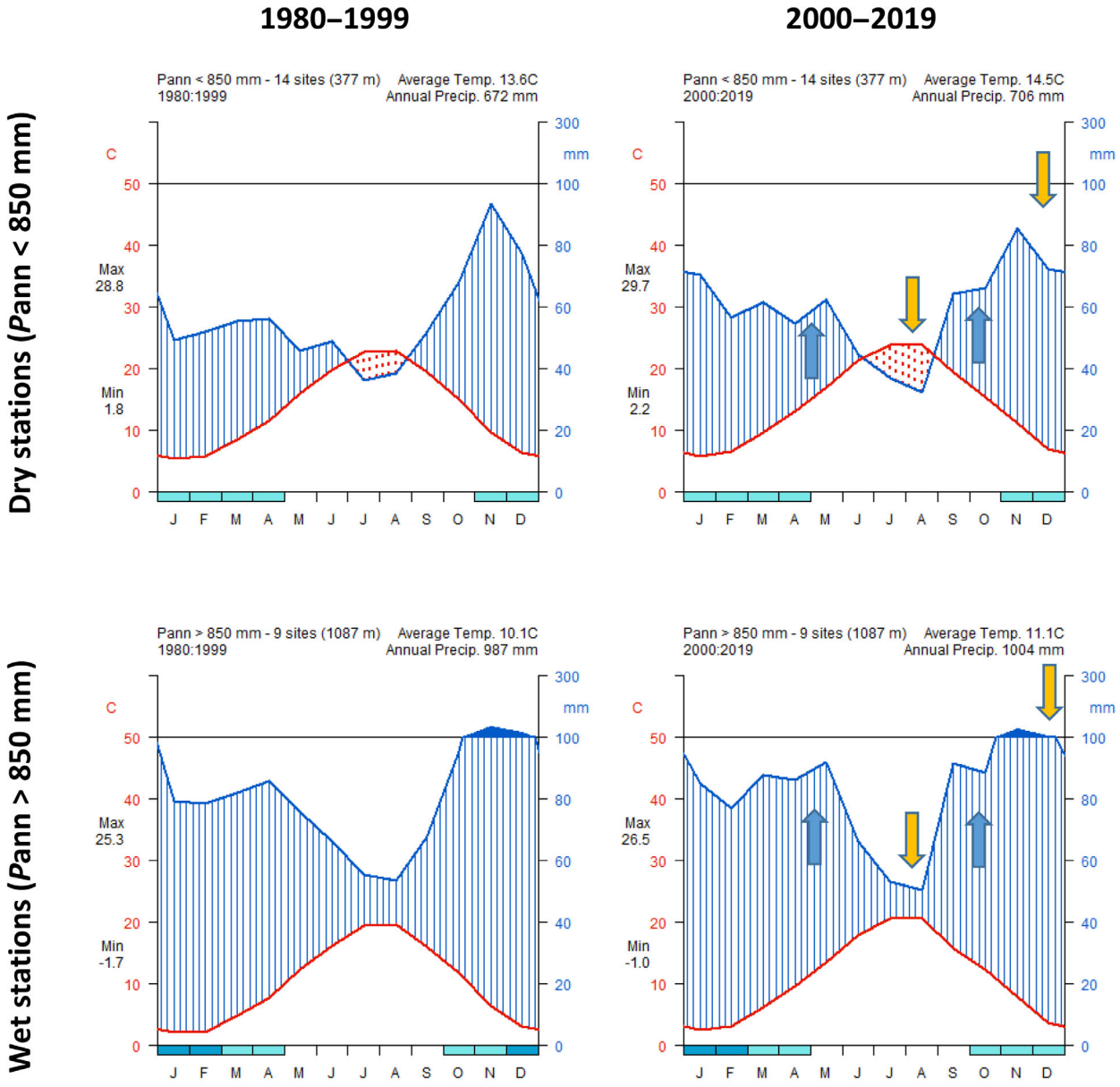

FIGURE 9 Walter-Lieth diagrams resulting from the average of two groups of stations: 'dry' and 'wet', defined as those station below or above 850 mm/year in the period 1980–2019. Two 20-years subperiods are compared: 1980–1999 on the left and 2000–2019 on the right [Colour figure can be viewed at wileyonlinelibrary.com]

3.6 | Sensitivity tests on the homogenization procedure

We carry out several sensitivity test on the homogenization procedure illustrated in Sections 2.3 and 3.1, in order to check the robustness of the obtained results.

The first test is aimed at elucidating the effect of the length of the period selected for the analysis in the detection of the breaks in the time series. This is relevant because different studies typically use different periods and because we expect a continuous update of the database with the inclusion of new data as time goes on. As reported in Section 3.1, over the period 1930–2019 we found a total number of breaks for the 42 stations equal to 236, 239 and 82 for TX, TN and RR, respectively. Considering the period 1930–2015 used by Aruffo and Di

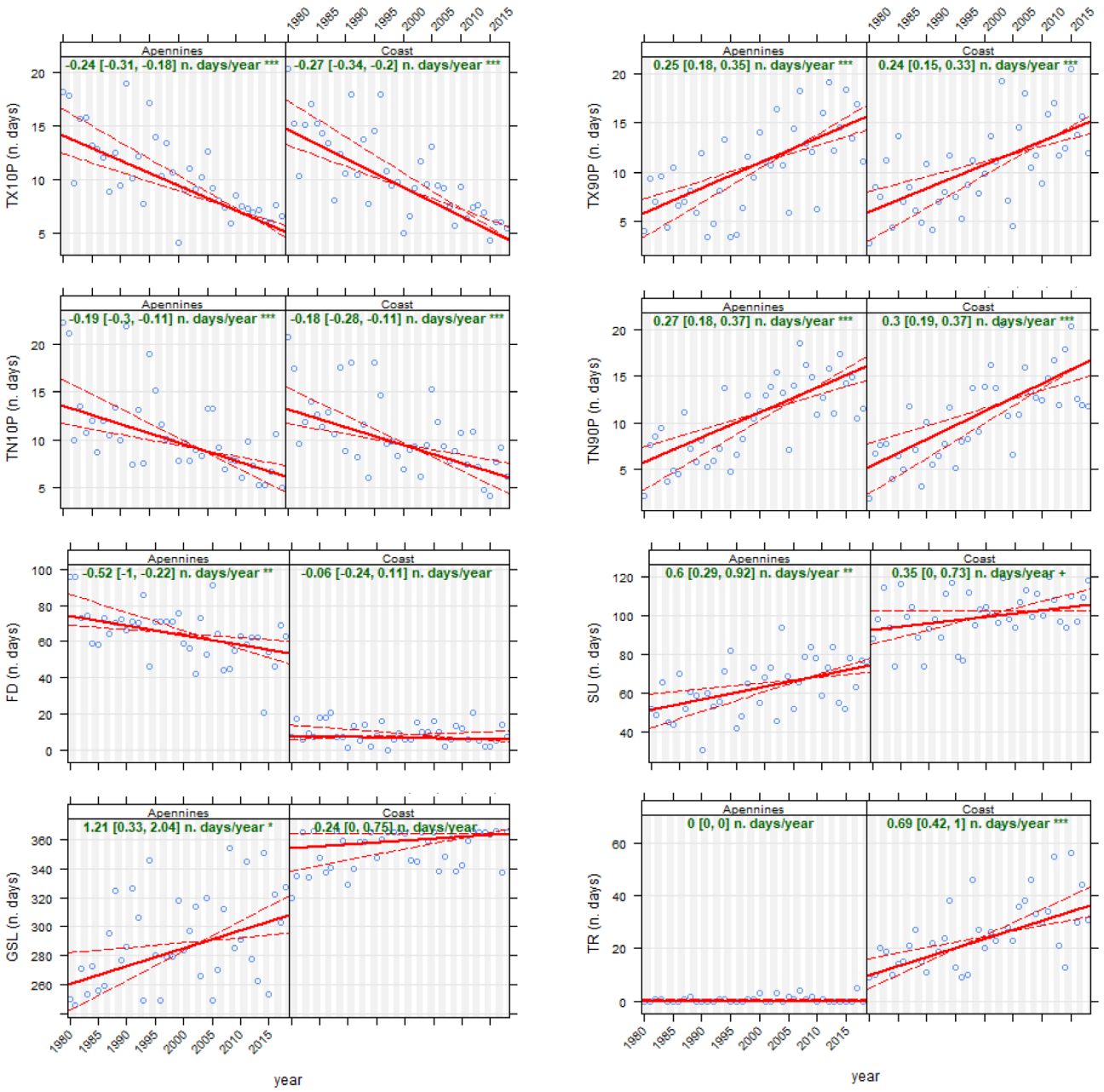

FIGURE 10 ETCCDI temperature-related climate indices aggregated for two groups of stations, 'Apennines' (western part of the region or altitude higher than 500 m) and 'Coast' (along the eastern part of the region). The climate indices denote: TX10p and TN10p the number of days with TX and TN less than the 10th percentile, TX90p and TN90p the number of days more than 90th percentile, FD n. of frost days (TN <0°C), SU n. summer days (TX >25°C), TR n. tropical nights (TN >20°C), GSL growing season length (period with daily mean temperature >6°C). The linear regression fit coefficients are shown inset, with significance (p <.001 = ***, p <.01 = **, p <.05 = * and p <0.1 = +) [Colour figure can be viewed at wileyonlinelibrary.com]

Carlo (2019), thus excluding the breaks in 2016–2019, the numbers are 223, 229 and 80. Re-running the procedure in the period 1930–2015, the resulting number of breaks is 218, 225 and 72. The order of magnitude is similar, but a decrease in the length of the series slightly reduces the sensitivity of the procedure in spotting the inhomogeneities. We repeated the exercise over the period 1980–2012 used by Scorzini *et al*. (2018). In the reference case we found 125, 126 and 39 breaks in the period 1980–2012, while re-running the procedure with input data from the period 1980–2012 we found 106, 112 and 27 breaks. The sensitivity of the break detection is sensibly reduced when using a consistently shorter time series: it is thus recommended to use the longest available time series for the homogenization.

The second test is aimed at clarifying the effect on the choice of the ensemble of stations. We repeated the procedure using the subset of 22 stations employed by Aruffo

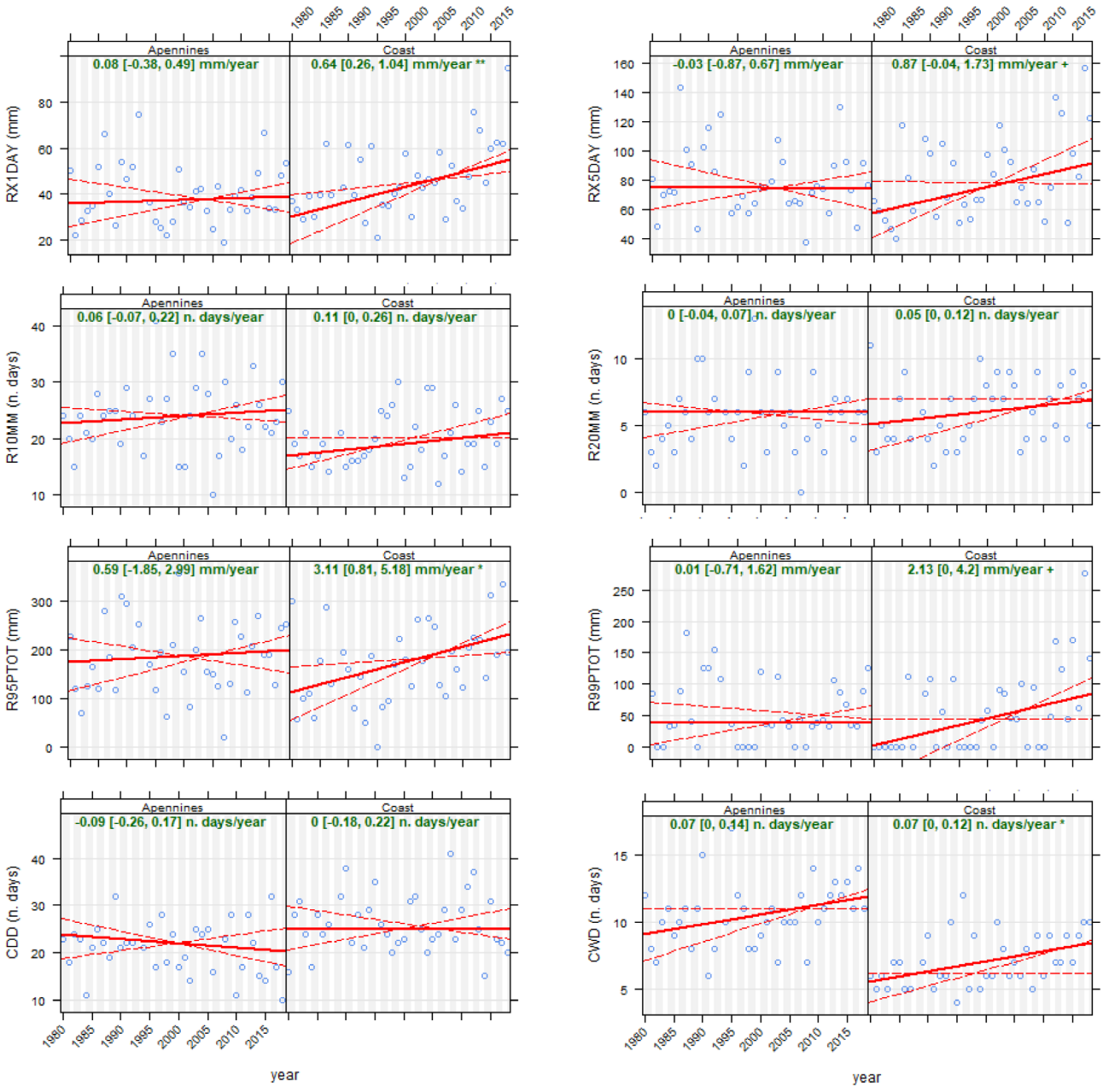

FIGURE 11 ETCCDI precipitation-related climate indices aggregated for the two groups of stations of Figure 10. The climate indices denote: Rx1day and Rx5day the maximum precipitation in 1-day and 5-days events, R10mm and R20mm the number of days with more than 10 and 20 mm of precipitation, R95pTOT and R99pTOT the total precipitation above the 95th and 99th percentile of daily rain, CDD and CWD are the maximum lengths of dry and wet spells. The linear regression fit coefficients are shown inset, with significance (p <.001 = ***, p <.01 = **, p <.05 = * and p <.1 = +) [Colour figure can be viewed at wileyonlinelibrary.com]

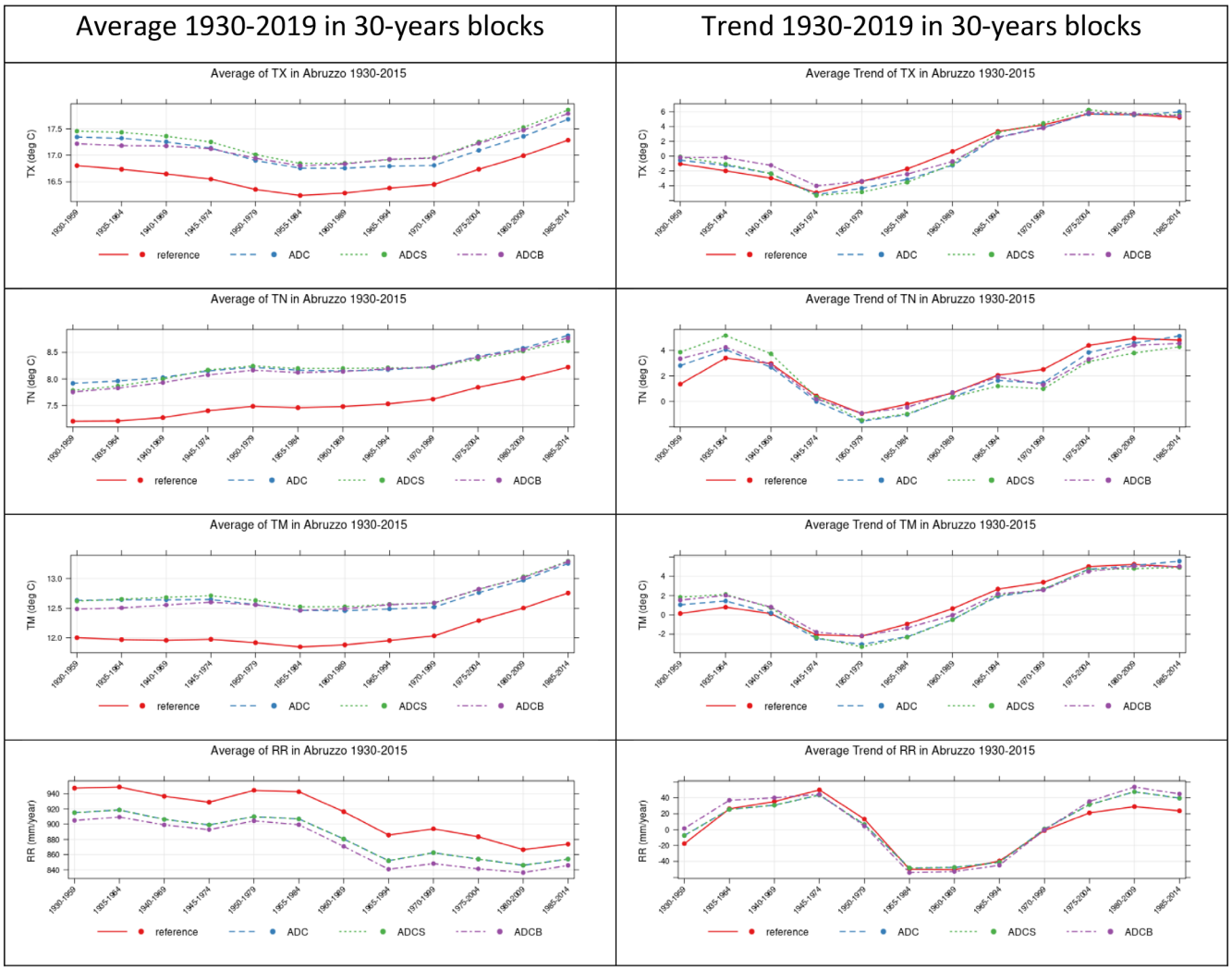

FIGURE 12 Comparison of average and trends in 30-years blocks (similar to Figure 5) over the period 1930–2019 for the sensitivity tests described in Table 2. Please note that the ensemble of stations used in the reference case is different from that used for sensitivity tests [Colour figure can be viewed at wileyonlinelibrary.com]

and Di Carlo (2019) over the period 1930–2015, because it is a longer range than that used by Scorzini *et al*. (2018). In our reference case, we found a total number of breaks for these 22 stations equal to 123, 124 and 21 for TX, TN and RR, respectively. Re-running the procedure using only the subset of the 22 stations, the number of breaks are 113, 127 and 15: the detection is thus slightly less sensitive. We also checked the dates of the breaks detected in both cases, and they differ at most by a few months (not shown). This result suggests that the identification of discontinuities is mainly determined by the comparison between the more continuous series.

In the third test, we illustrate the effect of different SNHT thresholds on break detection. We again use the independent work by Aruffo and Di Carlo (2019) as a term of comparison. In their work, the authors report a number of breaks detected for their set of 22 stations over the period 1930–2019 equal to 89 and 80 for TX and TN, respectively (they do not analyse RR), using a different homogenization tool (HOMER, see Section 2.3). As reported in the previous paragraph, with our Climatol-based procedure we detected 123 and 124 breaks. In Table S4, we already noted a generally higher number of breaks detected in our work in comparison to those detect by the other two studies (both using HOMER). Our default choice of SNHT thresholds, as reported in Section 3.1, is 30, 35 and 25 for TX, TN and RR, respectively. It evidently results in enhanced sensitivity to inhomogeneities with respect to the HOMER as used in previous studies. We performed several tests with increased SNHT values and found that the number of detected breaks actually decreases. For example, increasing by 10 the SNHT threshold and using the same 22 stations of Aruffo and Di Carlo (2019) over the period

TABLE 2 Sensitivity tests of homogenization procedure used for illustration of Figure 12

Case	Stations	Description
Reference	42 stations selected in this work	Reference case of this work, same as Figure 5
ADC	22 stations selected in the work of Aruffo and Di Carlo (2019)	Same settings of reference, but different subset of stations
ADCS	Same as ADC	Same as ADC, but SNHT thresholds for break detection increased by 10
ADCB	Same as ADC	Same as ADC, but using same predefined breaks reported by Aruffo and Di Carlo (2019)

1930–2015, we found a number of breaks equal to 87 and 75, which is similar to that reported by the authors.

In order to clarify the impact on the downstream results of the different details explored in the sensitivity tests for the homogenization procedure, we recalculated the average and trends illustrated in Figure 5 using the time series resulting from a selection of these tests. We added a further case to those discussed above, in order to verify the potential impact of a homogenization procedure other than Climatol, re-running the procedure using the list of breaks detected by Aruffo and Di Carlo (2019) (see their supporting information). The description of the cases is reported in Table 2, while the results are shown in Figure 5. The sensitivity tests are generally similar to each other and the larger differences are found between the reference case and the sensitivity tests. This implies that the selection of the subset of stations is the primary driver of the uncertainty in representing the average climate state over the region of interest. Focusing on the differences among the tests, we note that the averages are very similar, with differences of the order of tenths of degree for temperature and few mm/year for precipitation. On the other hand, the average trends display larger differences, especially in periods where there is a change in the direction of the slope and the absolute magnitude is not large, such as in the early part of the series for temperature and in the more recent part for precipitation. There, the differences are up to about 1%/century for temperature and 10%/century for precipitation, which is the same order of magnitude of the detected trend in that subperiods. Interestingly, the scatter among the sensitivity tests and also the reference case tends to sharply decrease when the magnitude of the trend is larger, such as in the most recent decades for temperature and in the middle of the series for precipitation. The recent warming appears to be a very robust signal emerging from the analysis.

4 | CONCLUSIONS

We built a reference climatological dataset for the analysis of temperature and precipitation trends over the Abruzzo region in Central Italy using monthly and daily time series in the period 1930–2019. The historical time series of Abruzzo have been analysed in recent studies (Aruffo & Di Carlo, 2019; Scorzini *et al*., 2018; Scorzini and Leopardi, 2019) and here we improve the past work under different aspects. We expanded the period of analysis from 1930 until 2019 for both temperature and precipitation series, and we employed a more up-to-date homogenization software that will facilitate both the technical sustainability and the further extension of the dataset, both in terms of update frequency and addition of new stations. We included and analyse within a single framework both the monthly and the daily timeseries from a historical perspective. Moreover, we added a station in the very western part of the region, strategic for agricultural practices (Burri and Petitta, 2004; Di Lena *et al*., 2018; Di Lena *et al*., 2019), which was not covered by the previously cited works. These new steps are aimed at following the path towards an improved local climate data rescue (WMO, 2016).

The time series correction procedure greatly reduced the unrealistic oscillations visible in the raw data and it resulted in trends more consistent with external observational datasets available at the global (CRU, Berkeley Earth) and European (E-OBS) scales. We tested the effect of several subjective choices, such as the length of the time series, the ensemble of considered stations, the statistical thresholds used to identify a break in the series, on the resulting homogenized dataset, and we verified that these choices imply little uncertainty when the trends of the variables are relatively large.

We derived a robust picture of the climate state and its trend in Abruzzo over the last century. We found, in broad agreement with previous studies, an increase of temperature and a decrease of precipitation on the long-term, partly offset by a positive trend in the recent decades. These trends are reflected in a visible shift of the Köppen–Geiger climate classification over the region. Comparing the periods 1930–1979 and 1970–2019, we found that the dry summer climates (Csa/Csb) became wetter temperate climate types (Cfa/Cfb) in the recent decades, in large parts of the valley in Apennines area and along the eastern coastal area. The total warm season precipitation increased due to rain in late spring and early autumn, although the precipitation in summer

months (JJA) actually decreased, as shown by the Walter–Lieth diagrams. Winter precipitation slightly decreased. Moreover, we observed a retreat of the cold climates of the mountain ranges, with wide bands around the slopes passing from Dfb to Cfb climate class.

A significant trend in the daily extreme values of temperature and precipitation is also found using daily time series in the period 1980–2019. The recent changes of climate extremes in the area and their connection with synoptic patterns were investigated in recent literature. Scorzini *et al*. (2018) found a high correlation of temperature indices with the East-Atlantic mode (Barnston and Livezey, 1987), which is usually associated with above-normal temperatures in Europe, while Scorzini and Leopardi (2019) reported that precipitation indices correlate with different circulation modes, also as a function of the topography of the region. The connection of changes observed within the extended dataset presented here could be used as a follow up of these studies.

The climate dataset built in this work constitutes a basic element for climate adaptation planning and climate change impact modelling over the Abruzzo region. The method may be readily implemented over other areas and updated with new time series at additional locations and for extended periods. Further development of this work will include the addition of more stations with relatively short but recent timeseries and the integration with operational medium-range and seasonal forecasts, in order to provide an even finer representation of the continuously evolving climate of the territory.

ACKNOWLEDGEMENTS

The authors thank 'Ufficio Idrografico e Maregrafico' and 'Centro Agrometeorologico Regionale' of Regione Abruzzo for kindly providing the observational dataset of temperature and precipitation over the region. Data analysis is carried out in the R environment (R Core Team, 2020) with RStudio GUI (RStudio Team, 2019), using the optional packages: climatol (Guijarro, 2019), openair (Ropkins and Carslaw, 2012), raster (Hijmans, 2020) and automap (Hiemstra *et al*., 2009).

ORCID

Gabriele Curci https://orcid.org/0000-0001-9871-5570
Anna Rita Scorzini https://orcid.org/0000-0002-5704-8481

REFERENCES

Aguilar, E., Auer, I., Brunet, M., Peterson, T.C. and Wieringa, J. (2003). *Guidelines on Climate Metadata and Homogenization*.

Alexandersson, H. (1986) A homogeneity test applied to precipitation data. *Journal of Climatology*, 6, 661–675. https://doi.org/10.1002/joc.3370060607.

Aruffo, E. and Di Carlo, P. (2019) Homogenization of instrumental time series of air temperature in Central Italy (1930-2015). *Climate Research*, 77, 193–204. https://doi.org/10.3354/cr01552.

Barnston, A.G. and Livezey, R.E. (1987) Classification, seasonality and persistence of low-frequency atmospheric circulation patterns. *Monthly Weather Review*, 115, 1083–1126. https://doi.org/10.1175/1520-0493(1987)115<1083:CSAPOL>2.0.CO;2.

Baronetti, A., González-Hidalgo, J.C., Vicente-Serrano, S.M., Acquaotta, F. and Fratianni, S. (2020) A weekly spatio-temporal distribution of drought events over the Po plain (North Italy) in the last five decades. *International Journal of Climatology*, 40, 4463–4476. https://doi.org/10.1002/joc.6467.

Beguería, S., Serrano-Notivoli, R. and Tomas-Burguera, M. (2018) Computation of rainfall erosivity from daily precipitation amounts. *Science of the Total Environment*, 637–638, 359–373. https://doi.org/10.1016/j.scitotenv.2018.04.400.

Brasseur, G.P. and Gallardo, L. (2018) Climate services: lessons learned and future prospects. *Reviews of Geophysics*, 4, 79–89. https://doi.org/10.1002/2015EF000338@10.1002/.

Brunetti, M., Maugeri, M., Monti, F. and Nanni, T. (2006) Temperature and precipitation variability in Italy in the last two centuries from homogenised instrumental time series. *International Journal of Climatology*, 26, 345–381. https://doi.org/10.1002/joc.1251.

Brunetti, M., Maugeri, M. and Nanni, T. (2000) Variations of temperature and precipitation in Italy from 1866 to 1995. *Theoretical and Applied Climatology*, 65, 165–174. https://doi.org/10.1007/s007040070041.

Brunetti, M., Maugeri, M., Nanni, T., Simolo, C. and Spinoni, J. (2014) High-resolution temperature climatology for Italy: interpolation method intercomparison: high-resolution temperature climatology for Italy. *International Journal of Climatology*, 34, 1278–1296. https://doi.org/10.1002/joc.3764.

Burri, E. and Petitta, M. (2004) Agricultural changes affecting water availability: from abundance to scarcity (Fucino plain, Central Italy). *Irrigation and Drainage*, 53, 287–299. https://doi.org/10.1002/ird.119.

Caporali, E., Lompi, M., Pacetti, T., Chiarello, V. and Fatichi, S. (2021) A review of studies on observed precipitation trends in Italy. *International Journal of Climatology*, 41, E1–E25. https://doi.org/10.1002/joc.6741.

CLC. (2018). *CLC 2018 — copernicus land monitoring service*. Available at: https://land.copernicus.eu/pan-european/corine-land-cover/clc2018.

Copernicus Climate Change Service, 2020. *E-OBS daily gridded meteorological data for Europe from 1950 to present derived from in-situ observations*. Available at: https://doi.org/10.24381/CDS.151D3EC6

Core Team, R. (2020) *R: A Language and Environment for Statistical Computing*. Vienna, Austria: R Foundation for Statistical Computing.

Cornes, R.C., van der Schrier, G., van den Besselaar, E.J.M. and Jones, P.D. (2018) An ensemble version of the E-OBS temperature and precipitation data sets. *Journal of Geophysical Research Atmospheres*, 123, 9391–9409. https://doi.org/10.1029/2017JD028200.

Di Lena, B., Farinelli, D., Palliotti, A., Poni, S., DeJong, T.M. and Tombesi, S. (2018) Impact of climate change on the possible expansion of almond cultivation area pole-ward: a case study of Abruzzo, Italy. *The Journal of Horticultural Science and*

Biotechnology, 93, 209–215. https://doi.org/10.1080/14620316.2017.1357433.

Di Lena, B., Silvestroni, O., Lanari, V. and Palliotti, A. (2019) Climate change effects on cv. Montepulciano in some wine-growing areas of the Abruzzi region (Italy). *Theoretical and Applied Climatology*, 136, 1145–1155. https://doi.org/10.1007/s00704-018-2545-y.

Durre, I., Menne, M.J., Gleason, B.E., Houston, T.G. and Vose, R.S. (2010) Comprehensive automated quality assurance of daily surface observations. *Journal of Applied Meteorology and Climatology*, 49, 1615–1633. https://doi.org/10.1175/2010JAMC2375.1.

ECA&D. (2013). European Climate Assessment & Dataset (ECA&D), Algorithm Theoretical Basis Document (ATBD), version 10.7.

ETCCDI. (1999). CCl/CLIVAR/JCOMM Expert Team (ET) on Climate Change Detection and Indices (ETCCDI) [WWW Document]. Available at: http://etccdi.pacificclimate.org/indices.shtml.

EU-DEM. (2020). EU-DEM v1.0, Copernicus Land Monitoring Service [WWW Document]. Available at: https://land.copernicus.eu/imagery-in-situ/eu-dem/eu-dem-v1-0-and-derived-products/eu-dem-v1.0.

European Environment Agency. (2006) *Land Accounts for Europe 1990–2000: Towards Integrated Land and Ecosystem Accounting, EEA Report*. Copenhagen: European Environment Agency.

Fioravanti, G., Fraschetti, P., Perconti, W., Piervitali, E. and Desiato, F. (2016). Controlli di qualità delle serie di temperatura e precipitazione.

Fioravanti, G., Piervitali, E. and Desiato, F. (2019) A new homogenized daily data set for temperature variability assessment in Italy. *International Journal of Climatology*, 39, 5635–5654. https://doi.org/10.1002/joc.6177.

Giorgi, F. (2019) Thirty years of regional climate modeling: where are we and where are we going next? *Journal of Geophysical Research Atmospheres*, 124, 5696–5723. https://doi.org/10.1029/2018JD030094.

Giorgi, F. and Lionello, P. (2008) Climate change projections for the Mediterranean region. *Global and Planetary Change*, 63, 90–104. https://doi.org/10.1016/j.gloplacha.2007.09.005.

Guijarro, J.A., 2019. climatol: Climate Tools (Series Homogenization and Derived Products).

Guijarro, J.A., Jansà, A., Campins, J., 2006. Time variability of cyclonic geostrophic circulation in the Mediterranean. In: *Advances in Geosciences. Presented at the 7th Plinius Conference on Mediterranean Storms (2005) - 7th Plinius Conference on Mediterranean Storms, Crete, Greece*, 5–7 *October 2005*, Copernicus GmbH, Vol. 7, pp. 45–49. https://doi.org/10.5194/adgeo-7-45-2006

Harris, I., Jones, P.D., Osborn, T.J. and Lister, D.H. (2014) Updated high-resolution grids of monthly climatic observations - the CRU TS3.10 dataset: updated high-resolution grids of monthly climatic observations. *International Journal of Climatology*, 34, 623–642. https://doi.org/10.1002/joc.3711.

Hiemstra, P.H., Pebesma, E.J., Twenhöfel, C.J.W. and Heuvelink, G.B.M. (2009) Real-time automatic interpolation of ambient gamma dose rates from the Dutch radioactivity monitoring network. *Computational Geosciences*, 35, 1711–1721. https://doi.org/10.1016/j.cageo.2008.10.011.

Hijmans, R.J. (2020). raster: geographic data analysis and modeling.

Hofstra, N., Haylock, M., New, M. and Jones, P.D. (2009) Testing E-OBS European high-resolution gridded data set of daily precipitation and surface temperature. *Journal of Geophysical Research Atmospheres*, 114. D21101. https://doi.org/10.1029/2009JD011799.

Köppen, W. (1884) The thermal zones of the earth according to the duration of hot, moderate and cold periods and of the impact of heat on the organic world. *Meteorologische Zeitschrift*, 1, 215–226.

Kottek, M., Grieser, J., Beck, C., Rudolf, B. and Rubel, F. (2006) World map of the Köppen-Geiger climate classification updated. *Meteorologische Zeitschrift*, 15, 259–263. https://doi.org/10.1127/0941-2948/2006/0130.

Kyselý, J. and Plavcová, E. (2010) A critical remark on the applicability of E-OBS European gridded temperature data set for validating control climate simulations. *Journal of Geophysical Research Atmospheres*, 115. D23118. https://doi.org/10.1029/2010JD014123.

Lai, S., Leone, F. and Zoppi, C. (2020) Spatial distribution of surface temperature and land cover: a study concerning Sardinia, Italy. *Sustainability*, 12, 3186. https://doi.org/10.3390/su12083186.

Maraun, D. (2016) Bias correcting climate change simulations - a critical review. *Current Climate Change Reports*, 2, 211–220. https://doi.org/10.1007/s40641-016-0050-x.

Mestre, O., Domonkos, P., Picard, F., Auer, I., Robin, S., Lebarbier, E., Böhm, R., Aguilar, E., Guijarro, J., Vertachnik, G., Klancar, M., Dubuisson, B. and Stepanek, P. (2013) HOMER: a homogenization software - methods and applications. *Idojaras*, 117, 47–67.

Peel, M.C., Finlayson, B.L. and McMahon, T.A. (2007) Updated world map of the Köppen-Geiger climate classification. *Hydrology and Earth System Sciences*, 11, 1633–1644. https://doi.org/10.5194/hess-11-1633-2007.

Peterson, T.C., Vose, R., Schmoyer, R. and Razuvaëv, V. (1998) Global historical climatology network (GHCN) quality control of monthly temperature data. *International Journal of Climatology*, 18, 1169–1179. https://doi.org/10.1002/(SICI)1097-0088(199809)18:11<1169::AID-JOC309>3.0.CO;2-U.

Ribeiro, S., Caineta, J. and Costa, A.C. (2016) Review and discussion of homogenisation methods for climate data. *Physics and Chemistry of the Earth, Parts A/B/C*, 94, 167–179. https://doi.org/10.1016/j.pce.2015.08.007.

Ropkins, K. and Carslaw, D.,.C. (2012) Openair - data analysis tools for the air quality community. *R J.*, 4, 20. https://doi.org/10.32614/RJ-2012-003.

RStudio Team. (2019) *RStudio: Integrated Development Environment for R*. Boston, MA: RStudio, Inc..

Rubel, F., Brugger, K., Haslinger, K. and Auer, I. (2017) The climate of the European Alps: shift of very high resolution Köppen-Geiger climate zones 1800–2100. *Meteorologische Zeitschrift*, 26, 115–125. https://doi.org/10.1127/metz/2016/0816.

Scorzini, A.R., Di Bacco, M. and Leopardi, M. (2018) Recent trends in daily temperature extremes over the central Adriatic region of Italy in a Mediterranean climatic context: temperature extremes over the central adriatic region of Italy. *International Journal of Climatology*, 38, e741–e757. https://doi.org/10.1002/joc.5403.

Scorzini, A.R. and Leopardi, M. (2019) Precipitation and temperature trends over Central Italy (Abruzzo region): 1951–2012.

Theoretical and Applied Climatology, 135, 959–977. https://doi.org/10.1007/s00704-018-2427-3.

Sen, P.K. (1968) Estimates of the regression coefficient based on Kendall's tau. *Journal of the American Statistical Association*, 63, 1379–1389. https://doi.org/10.1080/01621459.1968.10480934.

Venema, V.K.C., Mestre, O., Aguilar, E., Auer, I., Guijarro, J.A., Domonkos, P., Vertacnik, G., Szentimrey, T., Stepanek, P., Zahradnicek, P., Viarre, J., Müller-Westermeier, G., Lakatos, M., Williams, C.N., Menne, M.J., Lindau, R., Rasol, D., Rustemeier, E., Kolokythas, K., Marinova, T., Andresen, L., Acquaotta, F., Fratianni, S., Cheval, S., Klancar, M., Brunetti, M., Gruber, C., Prohom Duran, M., Likso, T., Esteban, P. and Brandsma, T. (2012) Benchmarking homogenization algorithms for monthly data. *Climate of the Past*, 8, 89–115. https://doi.org/10.5194/cp-8-89-2012.

Vicente-Serrano, S.M., Tomas-Burguera, M., Beguería, S., Reig, F., Latorre, B., Peña-Gallardo, M., Luna, M.Y., Morata, A. and González-Hidalgo, J.C. (2017) A high resolution dataset of drought indices for Spain. *Data*, 2, 22. https://doi.org/10.3390/data2030022.

Walter, H. and Lieth, H.H.F. (1967) *Klimadiagramm-Weltatlas*. Jena: G. Fischer Verlag.

Wijngaard, J.B., Klein Tank, A.M.G. and Können, G.P. (2003) Homogeneity of 20th century European daily temperature and precipitation series: homogeneity of European climate series. *International Journal of Climatology*, 23, 679–692. https://doi.org/10.1002/joc.906.

WMO, 2016. Guidelines on best practices for climate data rescue.

World Meteorological Organization. (2008) *Guide to meteorological instruments and methods of observation*. Geneva, Switzerland: World Meteorological Organization.

SUPPORTING INFORMATION

Additional supporting information may be found online in the Supporting Information section at the end of this article.

How to cite this article: Curci G, Guijarro JA, Di Antonio L, Di Bacco M, Di Lena B, Scorzini AR. Building a local climate reference dataset: Application to the Abruzzo region (Central Italy), 1930–2019. *Int J Climatol*. 2021;1–23. https://doi.org/10.1002/joc.7081